

# Turbulence in a three-dimensional deflagration model for type Ia supernovae: II. Intermittency and the deflagration-to-detonation transition probability

W. Schmidt

*Institut für Astrophysik, Universität Göttingen, Friedrich-Hund-Platz 1, D-37077  
Göttingen, Germany*

*and*

*Lehrstuhl für Astronomie und Astrophysik, Universität Würzburg, Am Hubland, D-97074  
Würzburg, Germany*

`schmidt@astro.physik.uni-goettingen.de`

F. Ciaraldi-Schoolmann

*Max-Planck-Institut für Astrophysik, Karl-Schwarzschild-Str. 1, D-85741 Garching,  
Germany*

*and*

*Lehrstuhl für Astronomie und Astrophysik, Universität Würzburg, Am Hubland, D-97074  
Würzburg, Germany*

J. C. Niemeyer

*Institut für Astrophysik, Universität Göttingen, Friedrich-Hund-Platz 1, D-37077  
Göttingen, Germany*

F. K. Röpke and W. Hillebrandt

*Max-Planck-Institut für Astrophysik, Karl-Schwarzschild-Str. 1, D-85741 Garching,  
Germany*

## ABSTRACT

The delayed detonation model describes the observational properties of the majority of type Ia supernovae very well. Using numerical data from a three-dimensional deflagration model for type Ia supernovae, the intermittency of the turbulent velocity field and its implications on the probability of a deflagration-to-detonation (DDT) transition are investigated. From structure functions of the

turbulent velocity fluctuations, we determine intermittency parameters based on the log-normal and the log-Poisson models. The bulk of turbulence in the ash regions appears to be less intermittent than predicted by the standard log-normal model and the She-L ev eque model. On the other hand, the analysis of the turbulent velocity fluctuations in the vicinity of the flame front by R opke suggests a much higher probability of large velocity fluctuations on the grid scale in comparison to the log-normal intermittency model. Following Pan et al., we computed probability density functions for a DDT for the different distributions. The determination of the total number of regions at the flame surface, in which DDTs can be triggered, enables us to estimate the total number of events. Assuming that a DDT can occur in the stirred flame regime, as proposed by Woosley et al., the log-normal model would imply a delayed detonation between 0.7 and 0.8 seconds after the beginning of the deflagration phase for the multi-spot ignition scenario used in the simulation. However, the probability drops to virtually zero if a DDT is further constrained by the requirement that the turbulent velocity fluctuations reach about  $500 \text{ km s}^{-1}$ . Under this condition, delayed detonations are only possible if the distribution of the velocity fluctuations is not log-normal. From our calculations follows that the distribution obtained by R opke allow for multiple DDTs around 0.8 seconds after ignition at a transition density close to  $1 \times 10^7 \text{ g cm}^{-3}$ .

*Subject headings:* stars: supernovae: individual: Ia — hydrodynamics — turbulence — methods: statistical

## 1. Introduction

Although deflagration models of Type Ia supernovae (e.g. Reinecke et al. 2002; Gamezo et al. 1991; R opke & Hillebrandt 2005) reproduce bulk properties of fainter Type Ia supernovae, delayed detonations (see Hillebrandt & Niemeyer 2000, for a review of explosion scenarios) seem to be the the most promising way of modeling the majority of the observed events (R opke & Niemeyer 2005; Mazzali et al. 2007).

However, a theoretical explanation for the deflagration-to-detonation (DDT) transition that gives rise to this type of thermonuclear explosion has been missing so far. Originally postulated by Khokhlov (1991) and Woosley & Weaver (1994), the possibility of a DDT in type Ia supernovae was questioned by Niemeyer (1999), because the preconditioning required to trigger a self-sustaining detonation front would be extremely unlikely to occur in the deflagration phase. This conclusion was based on ensemble-average scaling arguments. Pan et al.

(2008), on the other hand, pointed out that highly intermittent turbulent fluctuations act in favour of a DDT, because intermittency allows for velocities much higher than the ensemble average.

As proposed by Niemeyer & Woosley (1997), Niemeyer & Kerstein (1997) and Khokhlov et al. (1997), a necessary condition for triggering a DDT is that the distributed burning regime has to be entered. Based on log-normal (Kolmogorov 1962) and log-Poisson (She & Leveque 1994) intermittency models with typical parameters expected for turbulence in thermonuclear supernovae, Pan et al. calculated probabilities for this DDT condition. Their calculations implied transition densities in the range  $3.8 \times 10^7 \dots 2.7 \times 10^8 \text{ g cm}^{-3}$ . Lisewski et al. (2000), Woosley (2007), and Woosley et al. (2009), on the other hand, provided numerical evidence that there are stronger constraints on a DDT than just entering the regime of distributed burning. As a consequence, lower transition densities would be favored. Analyzing the small-scale turbulent velocity distribution predicted by the subgrid-scale model in several thermonuclear supernova simulations, Röpke (2007) found that intermittent velocity fluctuations up to  $1000 \text{ km s}^{-1}$  on a length scale of 10 km are possible. Fluctuations of this magnitude could trigger a detonation in accordance with Lisewski et al. (2000).

The ambiguity of conditions for DDTs in type Ia supernovae makes predictions difficult. Here, we follow a pragmatic approach and investigate different DDT criteria, assuming simple approximations to the microphysical conditions. Following the approach of Pan et al., we calculate the probability of a DDT using data sets from a highly resolved three-dimensional deflagration model (Röpke et al. 2007). Ciaraldi-Schoolmann et al. (2008), in the following referred to as paper I, determined characteristic scales and scaling exponents from the structure functions of the turbulent velocity fluctuations up to order six. We fitted log-normal and log-Poisson intermittency models to these scaling exponents. In addition, we determined probability density functions (pdfs) of the mass density constrained to the flame surface in order to calculate the probability of a DDT at different stages of the deflagration. There are no further adjustable parameters apart from the initial conditions of the deflagration model. Assuming a certain size for DDT regions, the total number of DDTs can be obtained from the cumulative probability and the number of regions in the volume occupied by the flame.<sup>1</sup>

Basically, Pan et al. (2008) assumed that a DDT is triggered once the Karlovitz number  $Ka$  (the square root of the ratio of the laminar flame width to the Gibson scale as defined in Section 3) exceeds a certain value (Niemeyer & Kerstein 1997; Woosley et al. 2009), i. e.,

---

<sup>1</sup> Down to the Gibson scale, the flame front can be considered as a fractal surface, which is numerically represented by a zero level set. Thus, the volume occupied by the flame is defined by all grid cells within a certain distance to the zero level set.

burning has advanced sufficiently far into the regime of distributed burning. Because the critical size of a preconditioned region is extremely sensitive to the mass density, it is difficult to estimate the total number of DDTs. Nevertheless, our results suggest that a delayed detonation would result at an early stage of the explosion if the conditions for a DDT were constrained by the Karlovitz number only. A further implication would be a transition density well above  $1 \times 10^7 \text{ g cm}^{-3}$ , which was found in the study by Pan et al. (2008).

Whereas the criterion for the onset of distributed burning can be expressed in terms of laminar flame properties, Woosley et al. (2009) argued that the conditions for a DDT cannot be parameterized on the basis of the laminar flame speed and thickness. Using numerical data for the nuclear time scale in the so-called stirred flame regime (Kerstein 2001) and following the same procedure as outlined above, we calculated the DDT probability. Although there are substantial uncertainties in this approach, a DDT at later time and lower density compared to the estimates following from laminar flame properties is implied. Most important, we find that a DDT can be excluded if the magnitude of the turbulent velocity fluctuations is required to exceed about  $500 \text{ km s}^{-1}$ , which is suggested by microphysical studies (Woosley 2007). Delayed detonations are possible, however, if the distribution of the velocity fluctuations significantly deviates from a log-normal shape. According to Röpke (2007), this appears to be the case for regions near the flame front.

The paper is organized as follows. In the next Section, we briefly review the log-normal and log-Poisson intermittency models. Moreover, the results on the intermittency of turbulence in the simulation are discussed. The procedure of calculating the DDT probability is described in Section 3. In Section 4, the estimation of the total number of DDTs is explained. We present our numerical results in this Section 5, followed by a discussion in the last Section.

## 2. Intermittency

According to the Kolmogorov theory of statistically stationary, homogeneous, and isotropic turbulence, the structure functions  $S_p(\ell) := \langle \delta v^p(\ell) \rangle$ , i. e., the ensemble average of the velocity fluctuations to the power  $p$  over a length scale  $\ell$ , follow power laws in the inertial subrange. The scaling exponents are given by  $\zeta_p = p/3$ . In several experiments, however, departures from the  $p/3$  scaling were found for higher-order structure functions. This phenomenon is attributed to the intermittency of turbulence (Frisch 1995, see). There are various theoretical intermittency models that predict anomalous scaling exponents. One example is the Kolmogorov-Oboukhov model (Kolmogorov 1962; Oboukhov 1962), which assumes a log-normal probability distribution function for the turbulent energy dissipation  $\epsilon_\ell$  on a length

scale  $\ell$ :

$$\text{pdf}(\ln(\epsilon_\ell/\epsilon)) = \frac{1}{\sqrt{2\pi\sigma_\ell^2}} \exp\left(-\frac{[\ln(\epsilon_\ell/\epsilon) + \sigma_\ell^2/2]^2}{2\sigma_\ell^2}\right), \quad (1)$$

where  $\epsilon$  is the mean rate of energy dissipation and  $\sigma_\ell^2 = \mu \ln(L/\ell)$  for the integral scale  $L$ . The scaling exponents resulting from this model are given by

$$\zeta_p^{(\text{ln})} = \frac{p}{3} - \frac{1}{18}\mu p(p-3), \quad (2)$$

where the parameter  $\mu$  is defined by  $\mu = 2 - \zeta_6$ . Experiments and simulations indicate  $\zeta_6 \approx 1.8$  and therefore  $\mu \approx 0.2$ . A deficiency of the log-normal model is that it fails to describe the observed higher-order scalings for  $p \geq 10$  (see Pan et al. (2008) for a detailed discussion of the limitations of this model). In this respect, the intermittency model by She & Leveque (1994) has been particularly successful:

$$\zeta_p^{(\text{SL})} = \frac{p}{9} + 2 \left[ 1 - \left(\frac{2}{3}\right)^{p/3} \right]. \quad (3)$$

Dubrulle (1994) and She & Waymire (1995) showed that this model can be accommodated within a two-parameter family of intermittency models, which are based on log-Poisson statistics:

$$\zeta_p^{(\text{IP})} = (1 - \Delta)\frac{p}{3} + \frac{\Delta}{1 - \beta} (1 - \beta^{p/3}) \quad (4)$$

The random cascade factor  $\beta \in [0, 1]$  specifies the degree of intermittency. Non-intermittent Kolmogorov scaling is obtained in the limit  $\beta \rightarrow 1$ . The parameter  $\Delta$  specifies the scaling properties of the most intermittent dissipative structures and is related to the codimension  $C$  of these structures:  $C = \Delta/(1 - \beta)$ . Setting  $\Delta = 2/3$  and  $\beta = 2/3$ , the She-Lévêque model (3) follows from equation (4). For these parameters, the codimension is  $C = 2$ . The interpretation is that vortex filaments are the most dissipative structures in subsonic turbulence (She & Leveque 1994). For supersonic turbulence,  $1 \leq C < 2$  because shock fronts also dissipate energy (Boldyrev et al. 2002; Kritsuk et al. 2007; Schmidt et al. 2009).

Equation (2) as well as (3) imply  $\zeta_3 = 1$  and, hence,  $S_3(\ell) \sim \epsilon\ell$ . In paper I, we determined the scaling exponents from power-law fits to the structure functions for  $p \leq 6$ . It was found that there is a transition length  $\ell_{\text{K/RT}} \sim 10$  km, where the radial second-order structure function changes from Kolmogorov scaling ( $S_2(\ell) \propto \ell^{2/3}$ ) to Rayleigh-Taylor scaling ( $S_2(\ell) \propto \ell$ ). The values of  $\ell_{\text{K/RT}}$  for  $t \geq 0.5$  seconds are listed in Table 1. While  $\zeta_3$  is approximately unity for the angular structure functions and also for the radial structure functions in the subrange  $\ell < \ell_{\text{K/RT}}$ , the radial third-order exponent for  $\ell > \ell_{\text{K/RT}}$  is about 1.5. On the other hand, it was shown in paper I that the relative scaling exponents  $Z_p =$

$\zeta_p/\zeta_3$  of the radial structure functions are nearly equal for the two subranges. However, since a consistent treatment of an exponent  $\zeta_3$  different from unity is highly non-trivial in the framework of the intermittency models mentioned above (Dubrulle 1994; Schmidt et al. 2008b), we do not consider the radial scaling exponents for length scales greater than  $\ell_{\text{K/RT}}$ . The values of  $\mu$  resulting from fits of the log-normal model to the exponents  $\zeta_p$  for  $t = 0.5, \dots, 0.9$  seconds are summarized in Table 1. Table 2 demonstrates that these values are consistent with  $\mu = 2 - \zeta_6$  within the error bars of the scaling exponents. For  $t = 0.7$  seconds, the scaling exponents of the radial and angular structure functions are plotted together with the fit functions in Figure 1. For comparison, also the log-normal model with  $\mu = 0.2$  and the She-Leveque model (3) are plotted. We find  $\mu \approx 0.1$ . Clearly, the numerical data from the supernova simulation indicate a lower degree of intermittency than these two models. Moreover, there is a remarkable agreement between the radial scaling exponents for the range of length scales  $\ell < \ell_{\text{K/RT}}$  and the scaling exponents of the angular structure functions over the whole range of length scales (also see paper I).

Fitting the general log-Poisson model (3) to the scaling exponents, yields ambiguous results. Pan et al. (2008) propose to set  $\Delta = 2/3$ . This appears to be a sensible choice on grounds of the hypothesis of a universal dissipation time scale, which determines  $\Delta$ . However, the best fits constrained by  $\Delta = 2/3$  imply a codimension greater than 2. Since it is hard to come up with a reasonable physical interpretation of this result, we tested the hypothesis  $C = 2$ , i. e., we consider the codimension of the most intense dissipative structure to be fixed. The resulting fit functions are almost indistinguishable from the best log-normal fits (see Figure 1). The log-Poisson fit parameters are also listed in Table 1. As one can see,  $\beta > 2/3$ , indicating a lower degree of intermittency in comparison to the She-Leveque model, and  $\Delta \approx 0.5$ . In this respect, the trend indicated by the log-normal model fits is confirmed. The anomalous intermittency parameters point at deviations from fully developed turbulence. A possible reason is that turbulence in supernova explosions does not reach a statistically stationary state. Since there are indications for  $\Delta > 2/3$  in the case of highly compressible turbulence (Schmidt et al. 2008b, 2009), the lower value of  $\Delta$  in the present case cannot be attributed to compressibility. Since the log-Poisson model is sensitive even to small errors in the higher-order scalings, the deviations from the She-Leveque model might be spurious. In this regard, however, one has to keep in mind that insufficiently converged statistics usually causes an *overestimate* of intermittency rather than an *underestimate* (see Frisch 1995).

Assuming that the low value of  $\mu$  is a peculiar property of non-stationary RT-driven turbulence in thermonuclear supernovae, one might raise the question if the small-scale isotropy discussed in paper I is genuine or, possibly, an artifact of the employed SGS model. Since our SGS model features a localized closure for the turbulence energy flux (Schmidt et al.

2006), isotropy on numerically resolved scales is not required. Only the unresolved turbulent velocity fluctuations are assumed to be isotropic. Fig. 2 in paper I demonstrates that the resolved velocity field is isotropic on length scales smaller than  $\ell_{\text{K/RT}}$ . At late time, when  $\ell_{\text{K/RT}}$  becomes less than the size of the grid cells, the radial and angular structure functions deviate even on the smallest numerically resolved scales and, thus, we have anisotropy on these scales. Consequently, isotropy does not appear to be forced by the SGS model if there is a pronounced anisotropy on length scales near the numerical cutoff scale. Although we cannot exclude the possibility that the SGS tends to make the nearby resolved scales more isotropic than in reality, because the interactions between resolved and unresolved scales are not strictly local, it is plausible that the observed isotropy on length scales  $\ell \lesssim \ell_{\text{K/RT}}$  is basically genuine.

Analyzing the statistics of the SGS velocity fluctuations in the vicinity of the flame front, Röpke (2007) found the high-velocity tail of the pdf is very well fitted by the expression  $\text{pdf}(\delta v(\ell)) = \exp[a_0 \delta v^{a_1}(\ell) + a_2]$  for  $\delta v(\ell) > 10^7 \text{ cm s}^{-1}$ , where  $\ell = \Delta$ . The local velocity fluctuation at the numerical cutoff is given by the specific SGS turbulence energy:  $\delta v(\Delta) = q_{\text{sgs}} = \sqrt{2k_{\text{sgs}}}$  (Schmidt et al. 2006). The coefficients  $a_0$ ,  $a_1$ , and  $a_2$  are fitted for each instant separately. The variation of the coefficients is due to the evolution of the turbulent flow. Changes might also result from the temporal shift of the cutoff scale. For the phase of the explosion we are interested in,  $\Delta$  is about 10 km, which in turn is close to  $\ell_{\text{K/RT}}$ . Further studies indicated that the above form of the pdf also holds for resolved velocity fluctuations on length scales  $\ell \sim \ell_{\text{K/RT}}$ . Thus, we assume that the fit coefficients do not change significantly for nearby scales at a fixed time. The corresponding pdf for  $\epsilon_\ell = \delta v^3(\ell)/\ell$  is given by

$$\text{pdf}(\epsilon_\ell) = \frac{\ell^{1/3}}{3\epsilon_\ell^{2/3}} \exp [a_0(\ell\epsilon_\ell)^{a_1/3} + a_2] \quad \text{for } \ell \sim 10 \text{ km.} \quad (5)$$

Fig. 1 in Röpke (2007) shows that the high-velocity tail is much flatter than the prediction of the log-normal intermittency model. Consequently, there appears to be a much higher degree of intermittency. It is important to note that this applies to velocity fluctuations at the flame surface. In this regard, the behavior of turbulence close to the flame front appears to be markedly different from the properties of the bulk of turbulence in ash regions, for which the log-normal fits to the scaling exponents imply a relatively *low* degree of intermittency. We will see in Section 5 that this difference is crucial for the occurrence of delayed detonations if tight constraints on DDTs are assumed.

### 3. Deflagration-to-detonation transition probability

Turbulent deflagration in the flamelet regime is characterized by a flame thickness  $\ell_{\text{fl}} < \ell_{\text{G}}$  (Niemeyer & Kerstein 1997), where the Gibson scale  $\ell_{\text{G}}$  is the length scale for which the turbulent velocity fluctuations are comparable to the laminar flame speed:  $\delta v(\ell_{\text{G}}) \sim s_{\text{lam}}$ . According to the refined similarity hypothesis of Kolmogorov (1962), we have  $\delta v(\ell) \sim \epsilon^{1/3} \ell^{1/3}$ . Assuming isotropic turbulence, the mean rate of dissipation  $\epsilon = V^3/L$ , where  $L$  and  $V$  are the integral length and the associated velocity, respectively. However, it was shown in paper I that turbulence in thermonuclear supernovae is anisotropic on length scales considerably smaller than  $L$ . We will therefore give a more precise definition below. In the ensemble average, it follows from  $\ell_{\text{G}} = (s_{\text{lam}}^3/V)^3 L$  that  $\epsilon \sim \text{Ka}^2 \epsilon_{\text{fl}}$ , where  $\epsilon_{\text{fl}} := s_{\text{lam}}^3/\ell_{\text{fl}}$  and the Karlovitz number  $\text{Ka} = (\ell_{\text{fl}}/\ell_{\text{G}})^{1/2}$  (Peters 2000). Once  $\ell_{\text{G}}$  becomes smaller than  $\ell_{\text{fl}}$ , i. e.,  $\text{Ka} > 1$ , distributed burning will commence (Niemeyer & Woosley 1997; Khokhlov et al. 1997). It should be noted that the meaning of  $\text{Ka}$  in terms of the Gibson length becomes elusive in the limit  $\text{Ka} \gg 1$ , because the flame thickness and the laminar burning speed are not well defined in this regime.

#### 3.1. Estimation of the DDT probability based on laminar flame properties

In log-normal as well as log-Poisson intermittency models, the rate of dissipation averaged over a region of size  $\ell$  is defined by a random variable  $\epsilon_{\ell}$  with a certain probability density function  $\text{pdf}(\epsilon_{\ell})$ . As pointed out by Pan et al. (2008), the probability of distributed burning with a certain Karlovitz number in a region of size  $\ell$  is then given by<sup>2</sup>

$$P(\epsilon_{\ell} > \text{Ka}^2 \epsilon_{\text{fl}}) = \int_{\text{Ka}^2 \epsilon_{\text{fl}}}^{\infty} \text{pdf}(\epsilon'_{\ell}) d\epsilon'_{\ell}. \quad (6)$$

As the Karlovitz number, for which a DDT can occur, increases, the probability given by the above equation declines. Apart from  $\text{Ka}$ , the threshold for  $\epsilon_{\ell}$  is given by laminar flame properties, because  $\epsilon_{\text{fl}}$  is defined by the speed and width of laminar flames.

Assuming that a DDT is caused by the Zel'dovich mechanism, there must be a sufficient number of preconditioned regions that reach the critical size  $\ell_c$ . This length scale depends on the mass density and the composition of the fuel (Niemeyer & Woosley 1997). While Pan et al. (2008) assumed a fixed density and a spherical flame, we evaluate the simulation data described in paper I. Specifically, we compute the effective probability that a single

---

<sup>2</sup>They use  $K = \text{Ka}^{2/3}$  as a fudge parameter, without referring to the Karlovitz number.

DDT occurs anywhere near the flame front from the convolution of the conditional probability  $P(\epsilon_\ell > \text{Ka}^2 \epsilon_{\text{fl}})$  with the normalized probability density function of the mass density  $\rho$  constrained to the flame front:

$$P_{\text{DDT}}(\text{Ka}) = \int_0^\infty P(\epsilon_{\ell_c} > \text{Ka}^2 \epsilon_{\text{fl}}) \text{pdf}(\rho|G=0) d\rho. \quad (7)$$

The flame front is numerically defined by the zero level set,  $G = 0$ , where  $G$  denotes the the level set function. Basically,  $G(t, \mathbf{r})$  is a distance function that is positive inside the flame (in ash regions) and negative outside. For the numerical calculation of  $\text{pdf}(\rho|G=0)$ , the grid cells in which  $G(t, \mathbf{r})$  switches sign are identified. The distribution of the mass density over the flame surface is mostly due to the density stratification in the exploding star. Since turbulence in SNe Ia is weakly compressible, we ignore correlations between local fluctuations of the density and the velocity.

For the calculation of  $P(\epsilon_{\ell_c} > \text{Ka}^2 \epsilon_{\text{fl}})$ , the probability density function of  $\epsilon_\ell$  has to be modelled. From the log-normal probability density function (1), the following expression for  $P(\epsilon_{\ell_c} > \text{Ka}^2 \epsilon_{\text{fl}})$  is obtained (Pan et al. 2008):

$$P(\epsilon_{\ell_c} > \text{Ka}^2 \epsilon_{\text{fl}}) = \frac{1}{2} \text{erfc} \left( \frac{\ln(\text{Ka}^2 \epsilon_{\text{fl}}/\epsilon)}{\sqrt{2}\sigma_{\ell_c}} + \frac{\sigma_{\ell_c}}{2\sqrt{2}} \right) \quad (8)$$

For the log-Poisson model, on the other hand, it is not possible to derive an analytic expression for  $P(\epsilon_c > \text{Ka}^2 \epsilon_{\text{fl}})$ , because the Poisson distributions contributing to  $\text{pdf}(\epsilon_\ell)$  are not explicitly known. For this reason, we will not consider the log-Poisson intermittency model in the following.

The restrictions of the log-normal model were discussed at length by Pan et al. (2008). Data from high-resolution simulations of turbulence suggest that the log-normal model yields a good approximation to the distribution of  $\epsilon_\ell$  within the  $5\sigma_\ell$  wings. However, it is not clear whether this range also applies to turbulence in thermonuclear supernova. A conservative estimate can be made as follows: Given a random variable  $X$ , the largest  $X$ -values, for which the probability density function  $\text{pdf}(X)$  is constrained by the moments of order  $\leq p$ , is indicated by the peak of  $X^p \text{pdf}(X)$ . Since  $\epsilon_\ell \sim \delta v^3(\ell)/\ell$ , we have  $\delta v^p(\ell) \text{pdf}(\delta v(\ell)) \sim \delta v^{p-1}(\ell) \text{pdf}(\ln[\delta v^3(\ell)/\ell\epsilon])$ , where the pdf on the right-hand side is defined by equation (1). We computed the scaling exponents of the structure functions up to sixth order. For  $\ell = 10 \text{ km}$  and the numerical parameters listed in Table 1,  $\delta v^6(\ell) \text{pdf}(\delta v(\ell))$  peaks for velocity fluctuations around  $100 \text{ km s}^{-1}$ , which corresponds to a range within  $2\sigma_\ell$  from the maximum of the log-normal  $\epsilon_\ell$ -pdf. Consequently, the model extrapolates the central part of the pdf, which can be inferred from the known structure functions, to the far tail. It is important to note that the range, for which the log-normal pdf is not well constrained by the scaling

exponents, is about the range of the asymptotic tail (5) resulting from the analysis of small-scale velocity fluctuations by Röpke (2007). In order to compare to the results of Pan et al. (2008), however, we will also consider a log-normal shape of the pdf up to  $5\sigma_\ell$ .

For the determination of the mean dissipation rate  $\epsilon$ , it is important to bear in mind that intermittency models such as the log-normal model apply to statistically isotropic turbulence. It was shown in paper I, that Kolmogorov scaling applies on length scales  $\ell < \ell_{\text{K/RT}}$ . For this reason, it is not correct to set  $\epsilon = V^3/L$ , where  $V$  and  $L$  are the scales of energy injection, in the case of RT-driven turbulence. In fact, the rate of dissipation is fixed by the transition length  $\ell_{\text{K/RT}}$  and the velocity scale  $\delta v(\ell_{\text{K/RT}})$ . Since the third-order structure function  $S_3(\ell) \simeq \epsilon \ell$ , we define  $\epsilon_{\text{rad}} := S_{3,\text{rad}}(\ell_{\text{K/RT}})/\ell_{\text{K/RT}}$ . However, one can also set  $\epsilon_{\text{ang}} := S_{3,\text{ang}}(L)/L$ , because the scaling of the angular structure function is unique and consistent with the Kolmogorov theory for the whole range of length scales. Table 1 gives an overview of the numerical values of  $\epsilon_{\text{rad}}$ ,  $\epsilon_{\text{ang}}$ , and  $L$  as functions of time. While both definitions yield similar results for the mean rate of dissipation, it is obvious from Figure 3 in paper I that  $\epsilon \ll V^3/L \sim S_{3,\text{rad}}(L)/L$  if  $V$  is taken to be the characteristic velocity of the Rayleigh-Taylor-driven turbulent flow at the length scale  $L$ . On the other hand, it is essential to set the integral length scale for the distribution of  $\epsilon_\ell$  to  $L$  rather than  $\ell_{\text{K/RT}}$ , because intermittent velocity fluctuations occur on all length scales  $\ell < L$ . Although turbulence is anisotropic for  $\ell_{\text{K/RT}} \lesssim \ell \lesssim L$ , we assume that the log-normal model can be applied to the whole range of length scales on the basis of the dissipation rate  $\epsilon_{\text{ang}} \simeq \epsilon_{\text{rad}}$ , because the angular structure functions continue to follow the scaling laws of isotropic turbulence for  $\ell > \ell_{\text{K/RT}}$ . In Section 5, we will carry out numerical calculations for both the radial and the angular parameter sets.

### 3.2. Estimation of the DDT probability in the stirred flame regime

So far, we have assumed that a DDT is only constrained by a value of  $\text{Ka}$  greater than unity. However, Woosley et al. (2009) argued that an additional requirement for a DDT is that  $\text{Da} > 1$ , where the Damköhler number  $\text{Da} = T/\tau_{\text{nuc}}$  is the ratio of a dynamical time scale  $T$  to the nuclear burning time scale  $\tau_{\text{nuc}}$  (Kerstein 2001). This regime is called the stirred flame (SF) regime. In the LEM study by Woosley et al. (2009), it was found that the size of a region, in which a detonation can be triggered, is about 10 km. Since the values of  $\ell_{\text{K/RT}}$  listed Table 1 are comparable to this size, we assume that  $\text{Da} \sim 1$  corresponds to a burning zone of size  $\sim \ell_{\text{K/RT}}$ . Then  $T = \ell_{\text{K/RT}}/\delta v(\ell_{\text{K/RT}})$  is the turn-over time of the largest eddies in the nearly isotropic regime. Since Kolmogorov scaling applies on length scales  $\ell \lesssim \ell_{\text{K/RT}}$ , it follows that  $T = \ell_{\text{K/RT}}^{2/3}/\epsilon$ . For  $\text{Da} > 1$ , there are broadened flame structures of

size smaller than  $\ell_{\text{K/RT}}$ .

In the framework of intermittency theory, the Damköhler number in a region of size  $\ell_{\text{K/RT}}$  is given by

$$\text{Da} = \frac{\ell_{\text{K/RT}}^{2/3}}{\epsilon_{\ell_{\text{K/RT}}}^{1/3} \tau_{\text{nuc}}}, \quad (9)$$

where  $\epsilon_{\ell_{\text{K/RT}}}$  is interpreted as the random dissipation rate on the length scale  $\ell_{\text{K/RT}}$ . Hence, the requirement  $\text{Da} > 1$  for a DDT in the SF regime corresponds to an *upper* bound on  $\epsilon_{\text{K/RT}}$ :

$$\epsilon_{\ell_{\text{K/RT}}} < \epsilon_{\text{WSR}} := \frac{\ell_{\text{K/RT}}^2}{\tau_{\text{nuc}}^3}. \quad (10)$$

If  $\text{Da}$  becomes less than unity ( $\epsilon_{\ell_{\text{K/RT}}} \geq \epsilon_{\text{WSR}}$ ), the well stirred reactor (WSR) regime is entered. In this regime, the density becomes so low that a detonation is very difficult and, eventually, the flames will be quenched.

On the other hand, if  $\text{Da}$  is yet too high, the broadened flames produced at the onset of distributed burning will be too sparse to coalesce into a mixed flame structure extending over  $\ell_{\text{K/RT}}$  (Woosley et al. 2009). For this reason, there is a *lower* bound on  $\epsilon_{\text{K/RT}}$  corresponding to a critical Damköhler number  $\text{Da}_{\text{crit}}$ :

$$\epsilon_{\ell_{\text{K/RT}}} > \epsilon_{\text{crit}} := \frac{\ell_{\text{K/RT}}^2}{\text{Da}_{\text{crit}}^3 \tau_{\text{nuc}}^3}. \quad (11)$$

If a DDT was only constrained by the range of  $\text{Da}$ , in principle, very small velocity fluctuations could trigger a delayed detonation at sufficiently low density because of the rapid increase of  $\tau_{\text{nuc}}$  as the bulk expansion causes the density to decrease. The mechanism of a DDT, however, is likely to require velocity fluctuations that reach a fraction  $\sim 0.1$  of the speed of sound (Lisewski et al. 2000; Woosley 2007). A typical figure for the minimal velocity fluctuation  $v'_{\text{min}}$  on length scales  $\ell \sim \ell_{\text{K/RT}} \sim 10 \text{ km}$  is  $500 \text{ km s}^{-1}$  (Woosley 2009).

Combining the constraints (11) and (10) with the requirement  $\epsilon_{\text{K/RT}} > \epsilon_{\text{min}} := (v'_{\text{min}})^3 / \ell_{\text{K/RT}}$ , the local probability of a DDT becomes

$$P \left( \epsilon_{\text{WSR}} > \epsilon_{\ell_{\text{K/RT}}} > \epsilon_{\text{crit}} \right) = \frac{1}{2} \text{erfc} \left[ \frac{\ln(\max(\epsilon_{\text{crit}}, \epsilon_{\text{min}})/\epsilon)}{\sqrt{2} \sigma_{\ell_{\text{K/RT}}}} + \frac{\sigma_{\ell_{\text{K/RT}}}}{2\sqrt{2}} \right] - \frac{1}{2} \text{erfc} \left[ \frac{\ln(\max(\epsilon_{\text{WSR}}, \epsilon_{\text{min}})/\epsilon)}{\sqrt{2} \sigma_{\ell_{\text{K/RT}}}} + \frac{\sigma_{\ell_{\text{K/RT}}}}{2\sqrt{2}} \right], \quad (12)$$

where  $\sigma_{\ell_{\text{K/RT}}} = \sqrt{\mu \ln(L/\ell_{\text{K/RT}})}$ . For the asymptotic pdf (5) proposed by Röpke (2007), on

the other hand, it follows that

$$P\left(\epsilon_{\text{WSR}} > \epsilon_{\ell_{\text{K/RT}}} > \epsilon_{\text{crit}}\right) = \frac{\exp(a_2)}{a_1(-a_0)^{1/a_1}} \times \left\{ \Gamma\left[\frac{1}{a_1}, -a_0(\max(\epsilon_{\text{WSR}}, \epsilon_{\text{min}})\ell)^{a_1/3}\right] - \Gamma\left[\frac{1}{a_1}, -a_0(\max(\epsilon_{\text{crit}}, \epsilon_{\text{min}})\ell)^{a_1/3}\right] \right\}. \quad (13)$$

The function  $\Gamma(x, y)$  is the incomplete gamma function.

As explained in Section 3.1, the effective DDT probability depending on  $\text{Da}_{\text{crit}}$  is

$$P_{\text{DDT}}(\text{Da}_{\text{crit}}) = \int_0^\infty P(\epsilon_{\text{WSR}} > \epsilon_{\ell_{\text{K/RT}}} > \epsilon_{\text{crit}}) \text{pdf}(\rho|G=0) d\rho. \quad (14)$$

The value of  $\text{Da}_{\text{crit}}$  has to be determined from microphysical studies. A reasonable range is  $10 \lesssim \text{Da}_{\text{crit}} \lesssim 100$  (Woosley 2009). Assuming that a DDT occurs at a transition density near  $1 \times 10^7 \text{ g cm}^{-3}$  in a region of size 10 km (Woosley et al. 2009),  $\epsilon_{\text{crit}} \sim 2.3 \times 10^{19} \text{ cm}^3 \text{ s}^{-2} / \text{Da}_{\text{crit}}^3$ . This is, even for  $\text{Da}_{\text{crit}} \sim 100$ , several orders of magnitude greater than  $\epsilon_{\text{fl}} \sim 1.1 \times 10^{10} \text{ cm}^3 \text{ s}^{-2}$ . Also note that  $\epsilon_{\text{min}} \sim 10^{17} \text{ cm}^3 \text{ s}^{-2}$  is higher than  $\epsilon_{\text{crit}}$  for  $\text{Da}_{\text{crit}} = 10$ . For this reason, the probability given by equation (14) is substantially more constrained than the probability  $P_{\text{DDT}}(\text{Ka})$  defined by (8). Detailed calculations are presented in the following Section.

#### 4. Number of deflagration-to-detonation transition events

In the previous Section, we obtained estimates of the effective probability of a DDT anywhere close to the flame surface. In order to assess whether a DDT is likely to occur at some instant, the expectation value  $N_{\text{DDT}}$  of the total number of events has to be calculated. Basically, this means that the effective DDT probability has to be multiplied with the number of regions of a certain size that can be accommodated within the burning zone. In this regard, it is important to account for the actual flame geometry, which becomes extremely folded and wrinkled in the course of the deflagration phase.

Specifying the DDT probability as a function of the Karlovitz number (see formula 8), we face the difficulty that the size  $\ell_c$  of a region, in which a detonation is triggered by the Zel'dovich mechanism, strongly varies with the mass density. For this reason, there is no simple relation between  $N_{\text{DDT}}$  and  $P_{\text{DDT}}(\text{Ka})$ . In order to calculate  $N_{\text{DDT}}$ , it would be necessary to weigh each  $d\rho$ -bin of  $\text{pdf}(\rho|G=0)$  with the number of regions of size  $\ell_c(\rho)$  contained in the volume of burning material at densities from  $\rho$  to  $\rho + d\rho$ . Since  $\ell_c$  is much smaller than the numerical resolution  $\Delta$  for  $\rho \gtrsim 10^7 \text{ g cm}^{-3}$ , this weighted distribution

cannot be inferred from the numerical data. Nevertheless, we can account for the flame geometry as far as it is numerically accessible by extrapolating the number of grid cells enveloping the flame front,  $N_\Delta$ , to the number  $N_c$  of critical regions of size  $\bar{\ell}_c$  given by the mean density of the burning material. If the fractal dimension of the flame front is  $D$ , it follows that  $N_c \sim N_\Delta(\Delta/\bar{\ell}_c)^D$ , and, thus, we estimate the total number of DDTs to be  $N_{\text{DDT}} \sim N_c P_{\text{DDT}}(\text{Ka})$ . Of course, the variation of the mass density over the flame surface at a given instant implies that  $N_c$  might be substantially different from  $N_\Delta(\Delta/\bar{\ell}_c)^D$  even for  $\bar{\ell}_c \sim \Delta$ . Nevertheless, once  $N_c P_{\text{DDT}}(\text{Ka})$  exceeds unity by a great margin, a DDT is likely to occur. Since the flame surface in type Ia supernovae is extremely wrinkled on length scales much smaller than the integral scale  $L$ , we tentatively set  $D = 3$ , i. e., the flame front is assumed to be space-filling.

For the DDT criterion of Woosley et al. (2009), on the other hand, an estimate of  $N_{\text{DDT}}$  is rather straightforward, because it is assumed that the size of regions, in which a DDT can be triggered, is given by  $\ell_{\text{K/RT}} \sim 10$  km. This length scale is independent of the mass density, and it is comparable to the size of the grid cells during the phase of the explosion we are interested in. Thus, we have  $N_{\text{DDT}} \sim N_{\text{K/RT}} P_{\text{DDT}}(\text{Da}_{\text{crit}})$ , where  $N_{\text{K/RT}} \sim N_\Delta(\Delta/\ell_{\text{K/RT}})^D$  and  $P_{\text{DDT}}(\text{Da}_{\text{crit}})$  is given by equation (14).

## 5. Numerical results

We interpolated  $\epsilon_{\text{fl}}$  from the numerical values of the laminar flame speed and the flame width (defined by the temperature profile) listed in Table 1 of Woosley et al. (2009) as a function of the mass density. Table 3 in the same article specifies values of the nuclear time scale  $\tau_{\text{nuc}}$  in the WSR regime for various densities. To estimate the critical length scale  $\ell_c$ , we made use of the compilation of data in Table 1 of Pan et al. (2008). Since there are only few values for different mass densities, the numerical evaluation of  $\ell_c$  is rather uncertain.

The resulting probability  $P(\epsilon_{\ell_c} > \epsilon_{\text{fl}})$  as function of the mass density for  $\text{Ka} = 1$  is shown in the Figure 2 for  $t = 0.6, 0.7, 0.8$  and  $0.9$  seconds. Except for the latest instant of time, the two solid curves were obtained by substitution of the parameters  $\mu$  and  $\epsilon$  inferred from the angular structure functions and the radial structure functions (see Table 1). The differences between both cases are small. This supports our assumption that the log-normal distribution can be determined on the basis of the the parameters  $\mu_{\text{ang}}$  and  $\epsilon_{\text{ang}}$  as well as  $\mu_{\text{rad}}$  and  $\epsilon_{\text{rad}}$ . This is important for  $t = 0.9$  seconds, where the regime of isotropic turbulence ( $\ell < \ell_{\text{K/RT}}$ ) is numerically unresolved, and we have only the parameters of the angular structure functions available. We find that  $P(\epsilon_{\ell_c} > \epsilon_{\text{fl}}) \simeq 1$  for  $\rho$  less than about  $2 \times 10^7 \text{ g cm}^{-3}$ . The probabilities assuming the time-independent models A, C and E (corresponding to  $\epsilon_{\text{fl}} = 10^{16}, 10^{14}$  and

$10^{12} \text{ cm}^2 \text{ s}^{-3}$ , respectively) of Pan et al. (2008) are indicated by the dashed lines in Figure 2. Our data fall in between models C and E. The steeper drop of the probability toward higher mass density in comparison to the models of Pan et al. is a consequence of the calculation of  $\epsilon_{\text{fl}}$  using the recent data by Woosley et al. (2009). Since it is considered to be more likely that a DDT occurs once the Karlovitz number becomes greater than 10 (Woosley et al. 2009), we also evaluated equation (8) for  $\text{Ka}^2 = 10, 100$  and  $1000$ . The resulting probabilities  $P(\epsilon_{\ell_c} > \text{Ka}^2 \epsilon_{\text{fl}})$  are plotted as functions of the mass density in Figure 3 for  $t = 0.9$  seconds. As one see, the range of densities for which  $P(\epsilon_{\ell_c} > \text{Ka}^2 \epsilon_{\text{fl}})$  is about unity decreases roughly by a factor of 2 as  $\text{Ka}^2$  is raised from 1 to 1000.

For the computation of the effective probability  $P_{\text{DDT}}(\text{Ka})$  as defined by equation (7), we substituted the probability density functions of the mass density constrained to the flame surface,  $\text{pdf}(\rho|G = 0)$ , which are plotted in Figure 4. Comparing Figures 2 and 4, it is evident that  $\text{pdf}(\rho|G = 0)$  significantly overlaps with  $P(\epsilon_{\ell_c} > \epsilon_{\text{fl}})$  as a function of density for  $t \geq 0.8$  seconds only. The product  $P(\epsilon_{\ell_c} > \epsilon_{\text{fl}}) \text{pdf}(\rho|G = 0)$  is shown in Figure 5 for  $t = 0.8$  and  $0.9$  seconds, and the effective probabilities obtained by integrating the probability densities are listed in Table 3. At time earlier than 0.8 seconds, the resulting probability of a DDT is low. For  $t = 0.8$  seconds,  $P_{\text{DDT}}$  would exceed 50%, if a DDT was triggered right at the onset of distributed burning ( $\text{Ka}=1$ ). We emphasize that this is a highly unrealistic assumption. However, effective probabilities higher than 50% result for all investigated values of  $\text{Ka}$  at time  $t = 0.9$  seconds.

Because of the huge number of regions of size  $\ell_c$  that can be accommodated within the flames, an order-of-magnitude estimate of  $N_c$  as outlined in Section 4 implies that  $N_{\text{DDT}}$  exceeds unity by many orders of magnitude already at  $t = 0.6$  seconds. At this time, the mass density at the flame front is of the order  $10^8 \text{ g cm}^{-3}$  (see Fig. 4), and  $\ell_c \sim 10^{-3} \text{ km}$  for this density. The number of grid cells of size  $\Delta \approx 4 \text{ km}$  is  $N_{\Delta} \sim 10^6$ . Hence,  $N_c \sim 10^{17}$  for  $D = 3$ , and with  $P_{\text{DDT}}(\text{Ka} = 1) \sim 10^{-7}$  (see Table 3), it follows that  $N_{\text{DDT}} \sim 10^{10}$ . For  $\text{Ka} = 10$ ,  $P_{\text{DDT}}(\text{Ka})$  decreases by a few orders of magnitude, but  $N_{\text{DDT}}$  is still much greater than unity. Even for  $D = 2$ ,  $N_c \sim 10^{13}$  and  $N_{\text{DDT}} \gg 1$  for  $\text{Ka} \lesssim 10$ . Thus, if the conditions for a DDT would be solely constrained by the Karlovitz number, delayed detonations could easily occur at early stages of the explosion.

The graphs of the local probability  $P(\epsilon_{\text{WSR}} > \epsilon_{\ell_{\text{K/RT}}} > \epsilon_{\text{crit}})$  according to the DDT constraints proposed by Woosley et al. (2009) are shown in Figure 6 for  $t = 0.8$  and  $0.9$  seconds. For comparison,  $P(\epsilon_{\ell_c} > \text{Ka}^2 \epsilon_{\text{fl}})$ , where  $\text{Ka} = 10^{3/2}$ , is also shown. As  $\text{Da}_{\text{crit}}$  decreases, the range of densities for which  $P(\epsilon_{\text{WSR}} > \epsilon_{\ell_{\text{K/RT}}} > \epsilon_{\text{crit}}) \sim 1$  becomes increasingly narrow. In contrast to  $P(\epsilon_{\ell_c} > \text{Ka}^2 \epsilon_{\text{fl}})$ , there is also a cutoff toward lower densities, which accounts for the fact that burning and, consequently, a DDT cannot occur at arbitrarily

low densities. However, the shape of this cutoff is largely qualitative, because it is based on extrapolations of the microphysical parameters in the range of densities lower than  $0.6 \times 10^7 \text{ g cm}^{-3}$ .

Calculating the DDT probability from equation (14) for critical Damköhler numbers in the range from  $10^{1/3}$  to 100, results in very small probabilities for  $t \leq 0.7$  seconds (see Table 4). From  $N_{\text{DDT}} \sim N_{\text{K/RT}} P_{\text{DDT}}(\text{Da}_{\text{crit}})$ , it follows that the expectation value of  $N_{\text{DDT}}$  is less than unity, except for  $\text{Da}_{\text{crit}} \geq 100$ . For  $t = 0.8$  and  $0.9$  seconds, on the other hand, the values of  $P_{\text{DDT}}(\text{Da}_{\text{crit}})$  are much higher and  $N_{\text{DDT}} \gg 1$  for all critical Damköhler numbers if we assume that there is no bound on the minimal velocity fluctuation (i. e.,  $\epsilon_{\text{min}} = 0$ ). Consequently, a delayed detonation would occur almost certainly between  $0.7$  and  $0.8$  seconds after ignition. The constrained probability density functions  $P(\epsilon_{\text{WSR}} > \epsilon_{\ell_{\text{K/RT}}} > \epsilon_{\text{crit}}) \text{pdf}(\rho|G = 0)$  plotted in Figure 7 allow us to assess the possible range of transition densities subject to the condition  $N_{\text{DDT}} \gtrsim 1$ . Depending on the value of  $\text{Da}_{\text{crit}}$ , transition densities ranging from  $0.5 \times 10^7$  to  $1.2 \times 10^7 \text{ g cm}^{-3}$  for  $t = 0.8$  seconds are most likely. For  $\text{Da}_{\text{crit}} = 10$  a transition density around  $0.7 \times 10^7 \text{ g cm}^{-3}$  would be preferred. Since  $N_{\text{DDT}} \sim 10^4$ , the transition density might be closer to  $10^7 \text{ g cm}^{-3}$  though. It is reassuring to note that our DDT densities are comparable to the ones determined from fits of 1D delayed detonation models to observational data. However, an exact match is not expected and would not necessarily lead to agreement of multi-dimensional models with observations because the detonation wave does not propagate spherically outwards.

However, the probability of a DDT drops dramatically if the minimal velocity to trigger a detonation,  $v'_{\text{min}}$ , is greater than about  $100 \text{ kms}^{-1}$ . In Table 5, the results for  $v'_{\text{min}} = 0, 200$  and  $500 \text{ kms}^{-1}$  are compared for different values of the intermittency parameter  $\mu$  at time  $t = 0.9$  seconds. As one can see, delayed detonations are virtually excluded if  $v'_{\text{min}} = 500 \text{ kms}^{-1}$ , as proposed by Woosley (2007). Assuming a smaller minimal velocity of  $200 \text{ kms}^{-1}$ , the results turn out to be extremely sensitive on the intermittency parameter  $\mu$ , while only small variation is found for  $v'_{\text{min}} = 0 \text{ kms}^{-1}$ . The reason becomes apparent from the dependence of the log-normal distribution on the intermittency parameter. In Figure 8, log-normal probability density functions for  $\ell = 10 \text{ km}$ ,  $\mu = 0.05, \dots, 0.2$ , and the parameters  $L$  and  $\epsilon$  determined by the angular structure functions at time  $t = 0.9$  seconds are plotted. Assuming  $\text{Da}_{\text{crit}} = 10$ , the thresholds  $\epsilon_{\text{crit}}$  defined by equation (11) are indicated for several different mass densities, which correspond to cumulative mass fractions of 20, 30, and 40% of burning material. If we solely consider the constraint  $\epsilon_{\text{WSR}} > \epsilon_{\ell} > \epsilon_{\text{crit}}$ , the intermittency parameter has only a small influence, because the cumulative probability is mainly determined by the central parts of the distributions. In the case that  $\epsilon_{\ell}$  must further satisfy, say,  $\epsilon_{\ell} > \epsilon_{\text{min}} = 8 \times 10^{15} \text{ cm}^3 \text{ s}^{-2}$  corresponding to  $v'_{\text{min}} = 200 \text{ kms}^{-1}$ , the cumulative probabilities are given by the right wings of the log-normal pdfs. Depending on the value

of  $\mu$ , there are substantial variations of the effective probabilities, as different portions of the wings contribute. If  $\epsilon_{\min}$  exceeds about  $10^{17} \text{ cm}^3 \text{ s}^{-2}$ , the probability of a DDT becomes virtually zero.

The asymptotic tails of the  $\epsilon_\ell$ -pdfs calculated by Röpke (2007), on the other hand, permit delayed detonations even for  $v'_{\min} = 500 \text{ kms}^{-1}$ . Table 6 summarizes the results for  $P_{\text{DDT}}$  and  $N_{\text{DDT}}$  at  $t = 0.7, 0.8$  and  $0.9$  seconds. For  $v'_{\min} = 500 \text{ kms}^{-1}$ , DDTs are likely to occur between  $0.7$  and  $0.8$  seconds. The constrained probability density function at  $t = 0.8$  seconds is plotted in the left panel of Fig. 9. The transition density for  $\text{Da}_{\text{crit}} = 10$  is close to  $1.0 \times 10^7 \text{ g cm}^{-3}$ . After  $0.8$  seconds the probabilities begin to decline because of the decreasing turbulence intensity (see Table 6 and the right panel of Fig. 9). This behavior is in marked contrast to the predictions based on lognormal distributions, for which the DDT probabilities at  $t = 0.9$  seconds are higher than for  $0.8$  seconds (see Table 4 and Fig. 7). Therefore, there appears to be a narrow time window, in which DDTs are possible. In Fig. 10, plots of  $\text{pdf}_{\text{DDT}}(\text{Da}_{\text{crit}})$  for  $t = 0.8$  seconds are shown for  $v'_{\min} = 200$  and  $1000 \text{ kms}^{-1}$ . It is obvious that the value of  $v'_{\min}$  has a huge impact on the probability density functions. As a consequence, delayed detonations could be set off earlier than  $0.7$  seconds after ignition if  $v_{\min}$  was about  $200 \text{ kms}^{-1}$  or less, whereas the DDT probabilities would be marginal for  $v'_{\min} = 1000 \text{ kms}^{-1}$ .

## 6. Conclusion

We investigated the intermittency properties of turbulence in the numerical simulation of a thermonuclear supernova by Röpke et al. (2007). Pan et al. (2008) proposed that the probability of entering the distributed burning regime can be computed from the log-normal model for intermittent turbulence, and from this probability the incidence of a DDT can be inferred. Evaluating the characteristic scales of turbulence and the probability density functions of the mass density in the vicinity of the flame front at different instants, we calculated the probability of a DDT for various Karlovitz numbers. We also investigated the influence of more restrictive criteria following from the numerical studies by Woosley et al. (2009).

Assuming that a detonation can be triggered after the onset of distributed burning, our calculations indicate that a delayed detonation would commence at an early stage of the explosion. In contrast to Pan et al. (2008), where a spherical flame is assumed, the highly wrinkled and folded flame front in the numerical simulation greatly increases the number of regions of critical size. Although we cannot precisely determine the total number of regions of size  $\ell_c$ , because the critical size greatly varies with the mass density (Niemeyer & Woosley

1997), and  $\ell_c \ll \Delta$ , where  $\Delta$  is the grid resolution, it appears that  $N_{\text{DDT}}$  greatly exceeds unity already 0.6 seconds after ignition. Then the transition density would be significantly higher than  $10^7 \text{ g cm}^{-3}$ . This possibility was pointed out by Pan et al. (2008).

If DDT conditions are constrained by an interval of Damköhler numbers in the stirred flame regime (Woosley et al. 2009), a DDT earlier than 0.7 seconds after ignition can be excluded. Assuming a typical value of the Damköhler number, for which a DDT can be triggered, a delayed detonation could occur around  $t = 0.8$  seconds, and the transition density would be close to  $10^7 \text{ g cm}^{-3}$ . However, assuming a log-normal distribution, the typical velocity fluctuations would be implausibly low. If turbulent velocity fluctuations greater than  $500 \text{ km s}^{-1}$  are required (Woosley 2009), then non-log-normal distributions are vital for delayed detonations.

One of the problems of determining log-normal distributions from scaling exponents of structure functions is that it is difficult to calculate higher-order two-point statistics. Consequently, the computed scaling exponents are sufficient to constrain the central part of the distribution only, whereas the tails are based on an extrapolation. A further caveat is that we are not able to separate ash from fuel regions, because two-point statistics of turbulence can only be computed in convex regions. For DDTs, however, turbulence in fuel close to the flame front is significant. Indeed, Röpke (2007) showed that the tail of the pdf of turbulent velocity fluctuations on a length scale of about 10 km in the vicinity of the flame front is much flatter than what is expected on the basis of log-normal models. With this distribution, DDTs between 0.7 and 0.8 seconds after ignition at a transition density close to  $10^7 \text{ g cm}^{-3}$  are definitely possible. Of course, the detonation time also depends on the ignition scenario and the subsequent evolution of the deflagration (see, for example, Schmidt & Niemeyer 2006). In any case, it is crucial to settle the question of the relevant distribution of turbulent velocity fluctuations in the future. Given a certain distribution, the minimal velocity fluctuation that is necessary to trigger a DDT is an extremely important parameter. Depending on this threshold, delayed detonations might be theoretically confirmed or excluded. Consequently, further studies of the microphysics, particularly in the range of densities below  $10^7 \text{ g cm}^{-3}$ , will be essential for a more accurate evaluation of the DDT probability in type Ia supernovae.

Based on the insights provided by such calculations, it may be possible to devise an algorithm that determines the local probability of a DDT in large-scale simulations of thermonuclear supernovae. Since the processes causing a DDT occur on scales that are difficult to resolve in such simulations, a subgrid scale model is likely to play some role (Schmidt et al. 2006). Apart from this, the propagation of the burning zone has to be treated beyond the onset of distributed burning. Schmidt (2007) proposed that the level set technique can be extended at least into the broken-reaction-zones regime (Kim & Menon 2000), provided that

the burning time scale does not exceed some fraction of the eddy turn-over time corresponding to the numerically unresolved velocity fluctuations (i. e., the ratio of the grid cell size to the square root of the specific subgrid scale turbulence energy). This approach also calls for further microphysical studies. An entirely different approach might be the use of adaptive mesh refinement and the *in situ* calculation of the processes triggering a DDT, for instance, by means of LEM (Kerstein 1991). Once all numerical challenges are met, quantitative theoretical arguments in favor or against delayed detonations as an explanation for type Ia supernovae will be within reach.

We are grateful to Stanford Woosley and Alan Kerstein for their comments and suggestions. The research of F. K. Röpke is supported through the Emmy Noether Program of the German Research Foundation (DFG; RO 3676/1-1) and by the Excellence Cluster “Origin and Structure of the Universe”.

## REFERENCES

- Boldyrev, S., Nordlund, Å., & Padoan, P. 2002, ApJ, 573, 678
- Ciaraldi-Schoolmann, F., Schmidt, W., Niemeyer, J. C., Röpke, F. K., & Hillebrandt, W. 2008, ApJ, in press (arXiv:0901.4254)
- Dubrulle, B. 1994, Physical Review Letters, 73, 959
- Frisch, U. 1995, Turbulence. The legacy of A.N. Kolmogorov (Cambridge: Cambridge University Press, 1995)
- Gamezo, V. N., Khokhlov, A. M., Oran, E. S., Chtchelkanova, A. Y., & Rosenberg, R. O. 2003, Science, 299, 77
- Hillebrandt, W. & Niemeyer, J. C. 2000, ARA&A, 38, 191
- Kerstein, A. R. 1991, J. Fluid Mech., 231, 361
- Kerstein, A. R. 2001, Phys. Rev. E, 64, 066306
- Khokhlov, A. M. 1991, A&A, 245, 114
- Khokhlov, A. M., Oran, E. S., & Wheeler, J. C. 1997, ApJ, 478, 678
- Kim, W., & Menon, S. 2000, Combust. Sci. Tech., 160, 119

- Kolmogorov, A. N. 1962, *Journal of Fluid Mechanics*, 13, 82
- Lisewski, A.M., Hillebrandt, W., & Woosley, S. E. 2000, *ApJ*, 538, 831
- Mazzali, P. A., Röpke, F. K., Benetti, S. & Hillebrandt, W. 2007, *Science*, 315, 825
- Niemeyer, J. C. 1999, *ApJ*, 523, L57
- Niemeyer, J. C. & Kerstein, A. R. 1997, *New Astronomy*, 2, 239
- Niemeyer, J. C. & Woosley, S. E. 1997, *ApJ*, 475, 740
- Kritsuk, A. G., Padoan, P., Wagner, R., & Norman, M. L. 2007, in *American Institute of Physics Conference Series*, Vol. 932, *Turbulence and Nonlinear Processes in Astrophysical Plasmas*, ed. D. Shaikh & G. P. Zank, 393
- Oboukhov, A. M. 1962, *Journal of Fluid Mechanics*, 13, 77
- Pan, L., Wheeler, J. C., & Scalo, J. 2008, *ApJ*, 681, 470
- Peters, N. 2000, *Turbulent Combustion* by Norbert Peters, pp. 320. Cambridge University Press
- Phillips, M. M., et al. 2007, *PASP*, 119, 360
- Reinecke, M., Hillebrandt, W., & Niemeyer, J. C. 2002, *A&A*, 391, 1167
- Röpke, F. K. 2007, *ApJ*, 668, 1103
- Röpke, F. K., & Hillebrandt, W. 2005, *A&A*, 431, 635
- Röpke, F. K., & Niemeyer, J. C. 2007, *A&A*, 464, 683
- Röpke, F. K., Hillebrandt, W., Schmidt, W., et al. 2007, *ApJ*, 668, 1132
- Schmidt, W. 2007, *A&A*, 465, 263
- Schmidt, W., Federrath, C., Hupp, M., Kern, S., & Niemeyer, J. C. 2009, *A&A*, 494, 127
- Schmidt, W., Federrath, C., & Klessen, R. 2008, *Physical Review Letters*, 101, 194505
- Schmidt, W., Niemeyer, J. C., & Hillebrandt, W. 2006, *A&A*, 450, 256
- Schmidt, W., Niemeyer, J. C., Hillebrandt, W., & Röpke, F. K. 2006, *A&A*, 450, 283
- Schmidt, W., & Niemeyer, J. C. 2006, *A&A*, 446, 627

- She, Z.-S. & Leveque, E. 1994, *Physical Review Letters*, 72, 336
- She, Z.-S. & Waymire, E. C. 1995, *Physical Review Letters*, 74, 262
- Timmes, F. X. & Woosley, S. E. 1992, *ApJ*, 396, 649
- Woosley, S. E. 2007, *ApJ*, 668, 1109
- Woosley, S. E. 2009, private communication
- Woosley, S. E., Kerstein, A. R., Sankaran, V. & Röpke, F. 2009, *ApJ*, submitted (arXiv:0811.3610)
- Woosley, S. E. & Weaver, T. A. 1994, in *Les Houches, Session LIV, Supernovae*, ed. S. A. Bludman, R. Mochkovitch, & J. Zinn-Justin (Amsterdam: North-Holland), 63

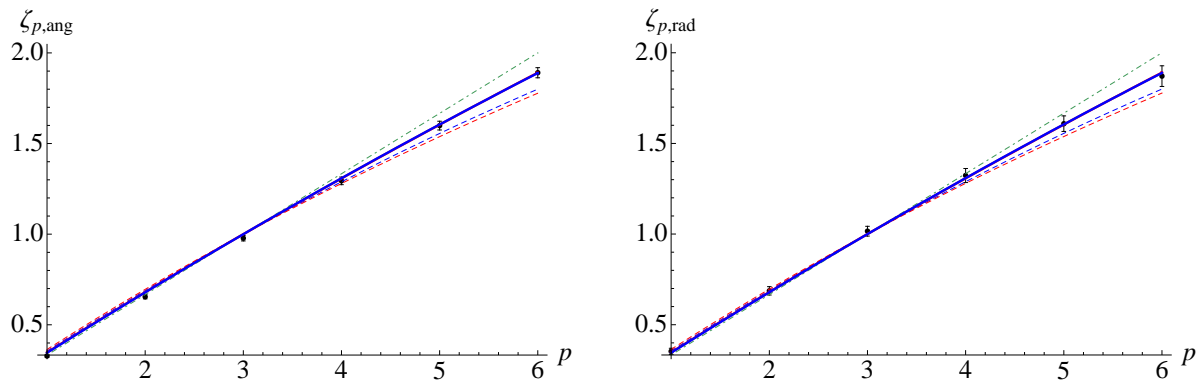


Fig. 1.— Scaling exponents of the angular (left) and radial (right) structure functions of order  $p \leq 6$  at time  $t = 0.7$  s. For comparison, the predictions of the Kolmogorov theory (dot-dashed line), the log-normal model (blue dashed line in the online version) with  $\mu = 0.2$  and the She-Leveque model (red dashed line in the online version) are plotted. The solid lines show the log-normal and log-Poisson fit functions, which are nearly coinciding. For the log-Poisson model, we set the codimension  $C = 2$ . The corresponding fit parameters are listed in Table 1.

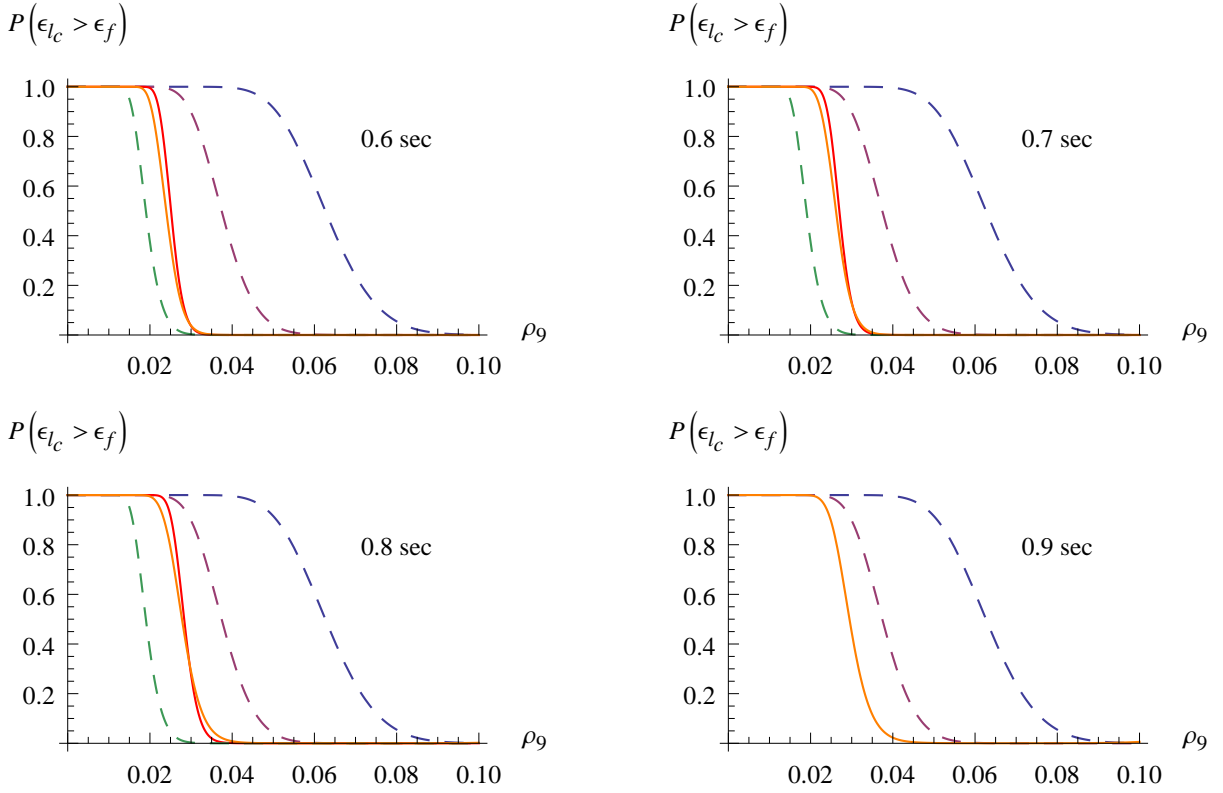


Fig. 2.— Dependence of the probability that the rate of dissipation  $\epsilon_{l_c}$  in a region of critical size  $l_c$  exceeds the threshold  $\epsilon_{fl}$  on the mass density for different stages of the explosion. For each instant, the results inferred from angular and radial structure functions (solid lines) are plotted together with three different models (A, C and E) of Pan et al. (2008). The mass density is specified in units of  $10^9 \text{ g cm}^{-3}$ .

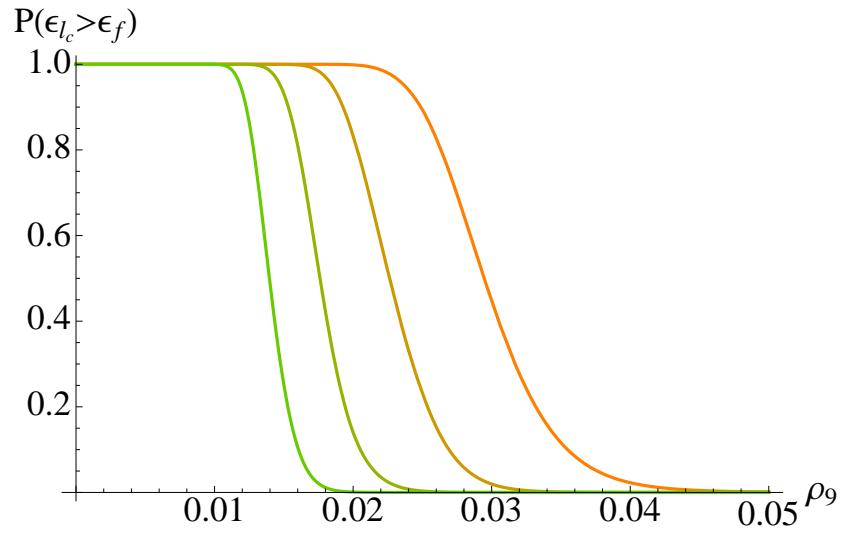


Fig. 3.— Variation of  $P(\epsilon_{l_c} > Ka^2 \epsilon_{fl})$  with the Karlovitz number  $Ka$  for  $t = 0.9$  seconds. From right to left, the curves correspond to  $Ka^2 = 1, 10, 100$  and  $1000$ . The mass density is specified in units of  $10^9 \text{ g cm}^{-3}$ .

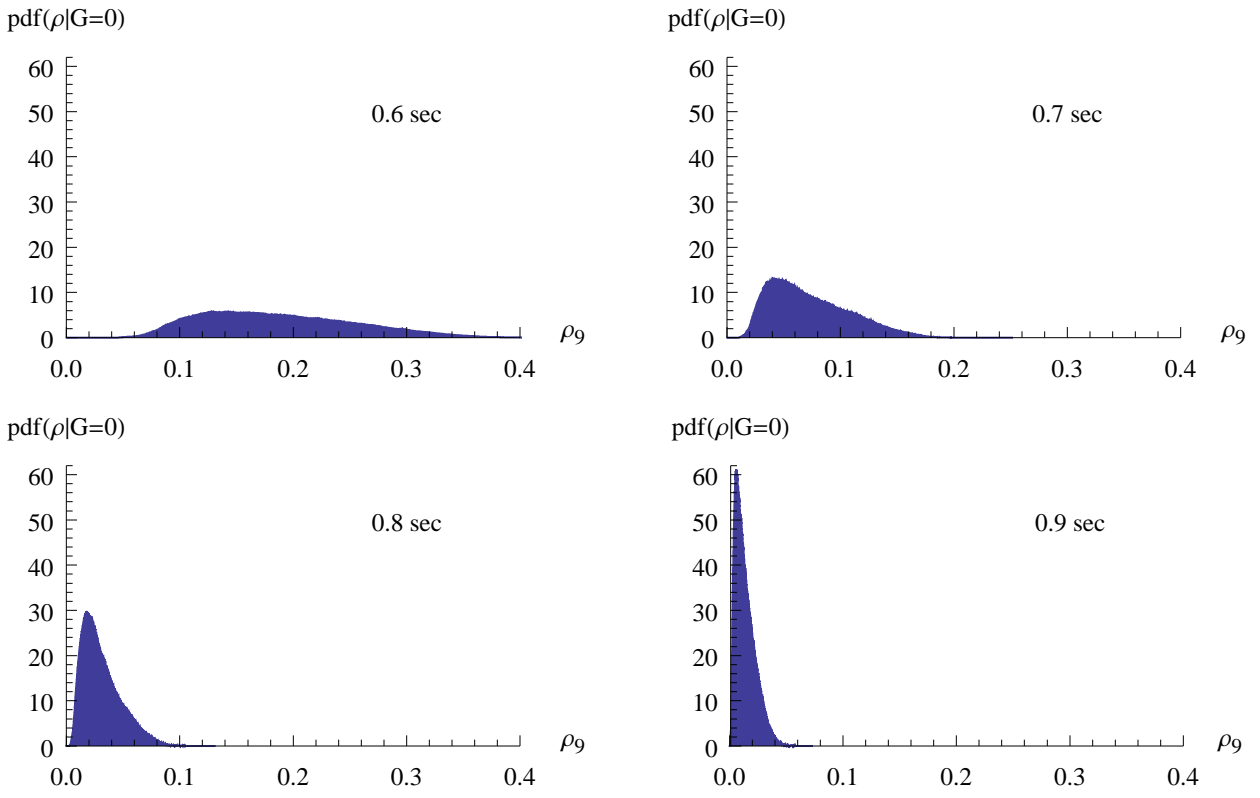


Fig. 4.— Probability density functions of the mass density constrained to the flame front at different instants. The mass density is specified in units of  $10^9 \text{ g cm}^{-3}$ .

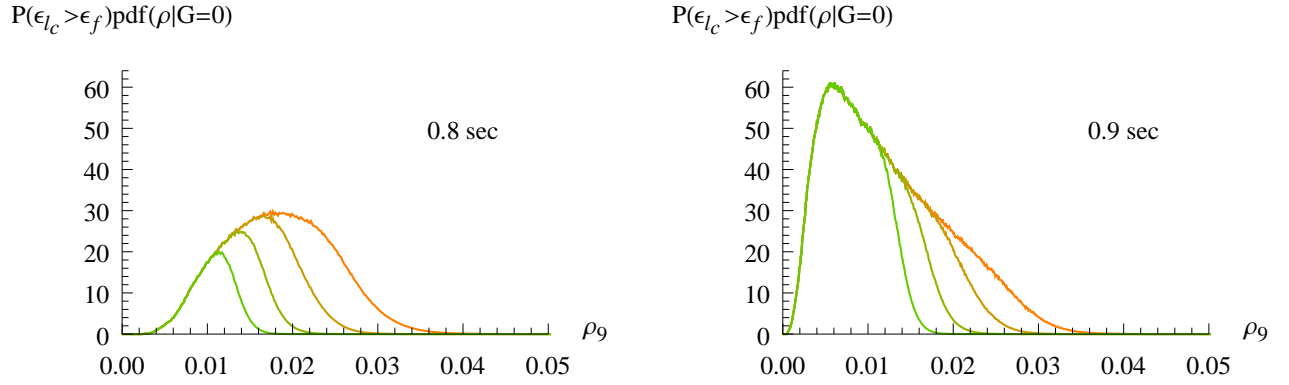


Fig. 5.— Constrained probability density functions for triggering a DDT by velocity fluctuations satisfying  $\epsilon_{l_c} > \text{Ka}^2 \epsilon_{fl}$  for  $t = 0.8$  (left) and  $0.9$  (right) seconds. For  $\text{Ka}^2$  increasing from 1 to 1000 by factors of 10, the distribution becomes increasingly narrow. The calculation is based on the parameters  $\mu$  and  $\epsilon$  obtained from the angular structure functions. The mass density is specified in units of  $10^9 \text{ g cm}^{-3}$ .

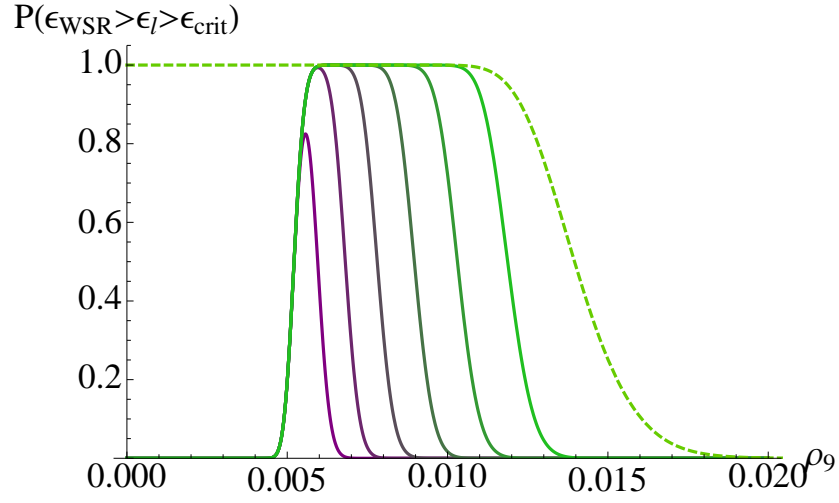


Fig. 6.— Variation of  $P(\epsilon_{\text{WSR}} > \epsilon_l > \epsilon_{\text{crit}})$  with the critical Damköhler number,  $\text{Da}_{\text{crit}}$ , for  $\ell = 10$  km at time  $t = 0.9$  seconds. The distribution becomes increasingly narrow as  $\text{Da}_{\text{crit}}^3$  decreases from  $10^6$  to  $10$  in order-of-magnitude steps. For comparison,  $P(\epsilon_{\ell_c} > 1000\epsilon_{\text{fl}})$  is shown as dashed curve. The mass density is specified in units of  $10^9 \text{ g cm}^{-3}$ .

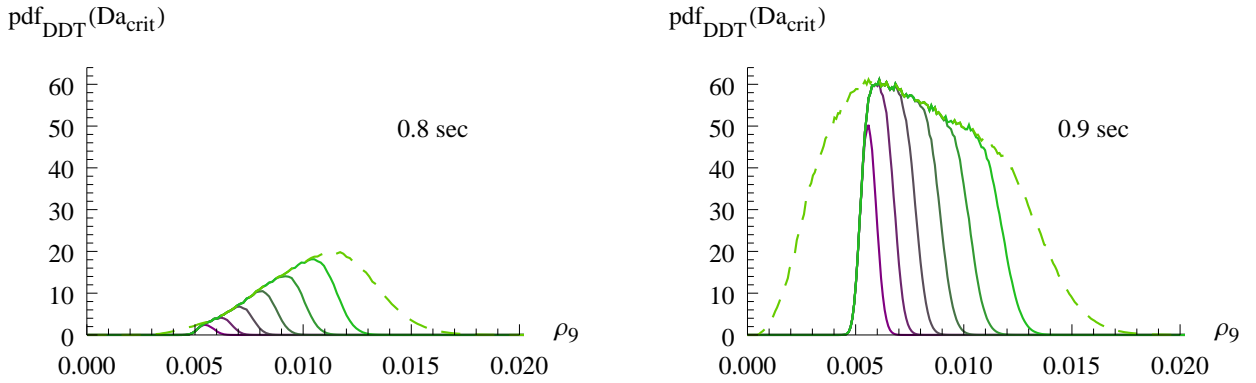


Fig. 7.— Constrained probability density functions for triggering a DDT by velocity fluctuations satisfying  $\epsilon_{\text{WSR}} > \epsilon_\ell > \epsilon_{\text{crit}}$  for  $\ell = 10$  km at time  $t = 0.8$  (left) and  $0.9$  (right) seconds, where the solid curves correspond to  $\text{Da}_{\text{crit}}^3$  decreasing from  $10^6$  to  $10$  in order-of-magnitude steps from right to left. The constrained PDF resulting from the criterion  $\epsilon_{\ell_c} > 1000\epsilon_{\text{fl}}$  is indicated by the dashed line. The calculation is based on the parameters  $\mu$  and  $\epsilon$  obtained from the angular structure functions. The mass density is specified in units of  $10^9 \text{ g cm}^{-3}$ .

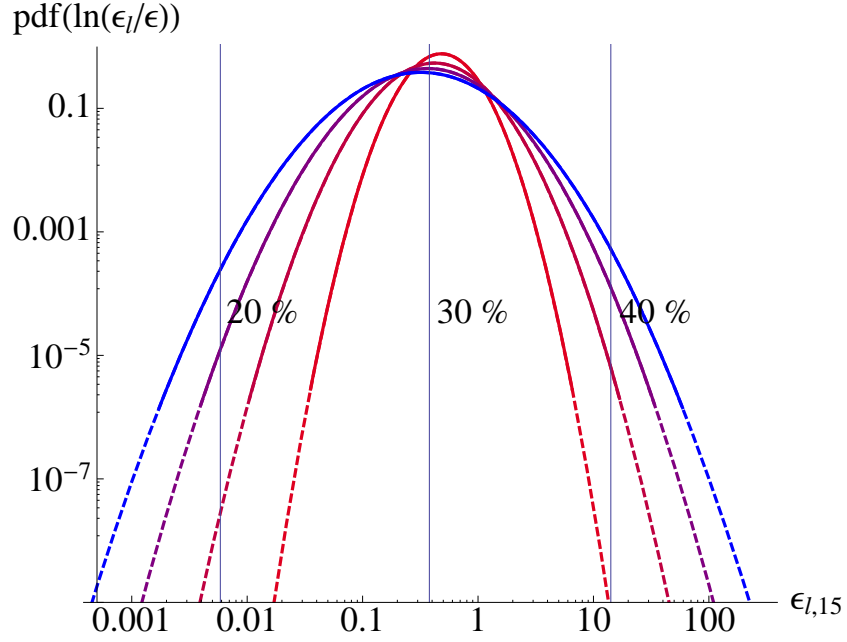


Fig. 8.— Log-normal probability density functions (1) of  $\epsilon_\ell$  in units of  $10^{15} \text{ cm}^3 \text{ s}^{-2}$  for  $\ell = 10 \text{ km}$  at time  $t = 0.9$  seconds. The mean rate of dissipation  $\epsilon$  and the integral scale  $L$  are determined by the third-order angular structure functions (see Table 1). The four plotted pdfs follow for  $mu = 0.05$  (most narrow distribution), 0.1, 0.15, and 0.2 (widest distribution). The tails beyond  $5\sigma_\ell$  are dashed. The vertical lines indicate the values of  $\epsilon_{\text{crit}}$  defined by equation (11) for different mass densities, assuming that the critical Damköhler number is equal to 10. The percentages indicate the volume fractions of matter at densities less than the mass densities chosen for the evaluation of  $\epsilon_{\text{crit}}$ .

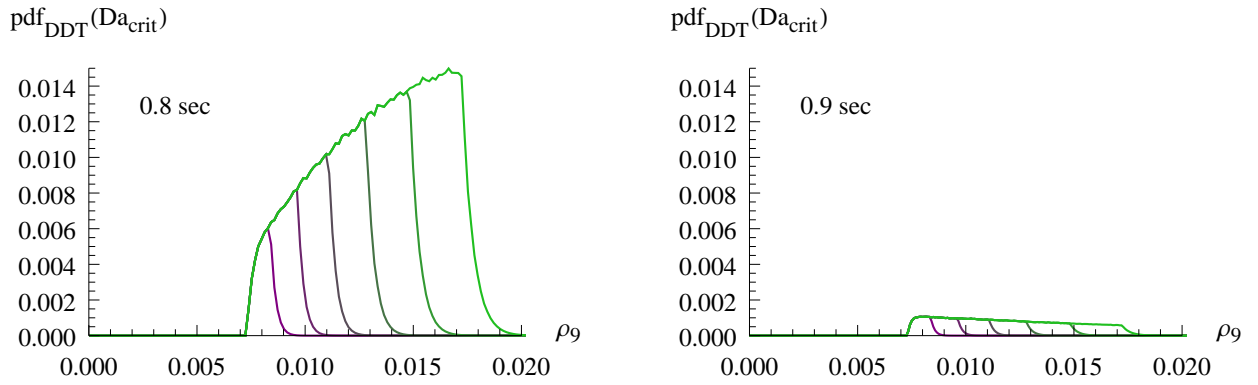


Fig. 9.— The same probability density functions as in Figure 7, however, with the local DDT probability given by equation (13) in place of (12), and  $v'_{\text{min}} = 500 \text{ km s}^{-1}$ . Note that the ordinate scale is different from Figure 7.

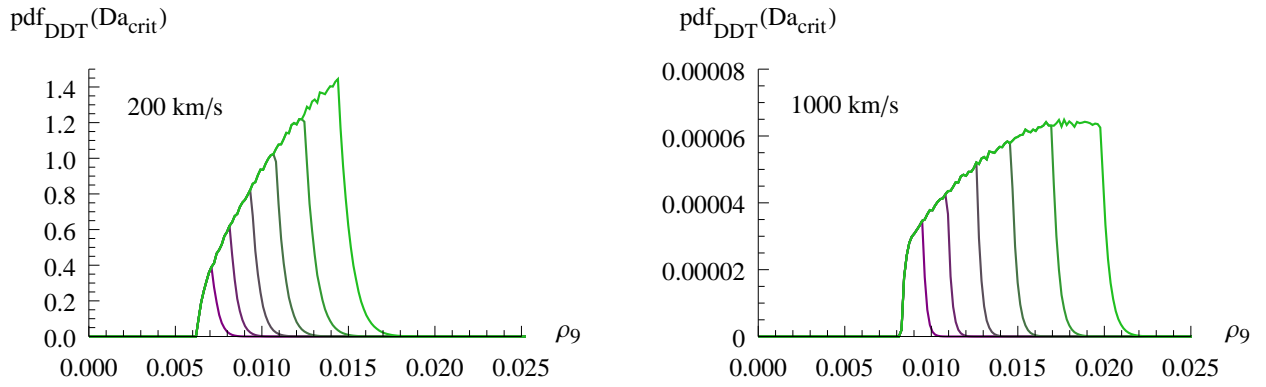


Fig. 10.— Variation of the probability density functions shown in the left panel of Fig. 9 for  $v'_{\text{min}} = 200 \text{ km s}^{-1}$  (left) and  $v'_{\text{min}} = 1000 \text{ km s}^{-1}$  (right). Note that the different ordinate scales.

$t$ [s]	$L$	$l_{K/RT}$	$\epsilon_{\text{ang}}$	$\epsilon_{\text{rad}}$	$\mu_{\text{ang}}$	$\mu_{\text{rad}}$	$\beta_{\text{ang}}$	$\beta_{\text{rad}}$	$\Delta_{\text{ang}}$	$\Delta_{\text{rad}}$
0.5	516	15.4	0.0332	0.0634	0.096	0.139	0.783	0.738	0.434	0.523
0.6	799	14.4	0.0819	0.0972	0.128	0.134	0.750	0.744	0.501	0.512
0.7	1023	14.3	0.166	0.177	0.111	0.121	0.766	0.755	0.468	0.489
0.8	1578	12.9	0.335	0.274	0.140	0.128	0.738	0.749	0.525	0.503
0.9	2324	...	0.551	...	0.132	...	0.745	...	0.510	...

Table 1: Parameters of log-normal and log-Poisson model fits to the angular and radial scaling exponents at different instants. The radial scalings apply to the subrange  $\ell < \ell_{K/RT}$ . Also specified are the integral scale and the mean rate of dissipation inferred from the radial and angular structure functions.

$t$ [s]	$\mu_{\text{ang}}$	$2 - \zeta_{6,\text{ang}}$	$\text{std}(\zeta_{6,\text{ang}})$	$\mu_{\text{rad}}$	$2 - \zeta_{6,\text{rad}}$	$\text{std}(\zeta_{6,\text{rad}})$
0.5	0.096	0.099	0.037	0.139	0.144	0.047
0.6	0.128	0.125	0.033	0.134	0.141	0.055
0.7	0.111	0.109	0.028	0.121	0.129	0.057
0.8	0.140	0.141	0.044	0.128	0.134	0.054
0.9	0.132	0.132	0.043	...	...	...

Table 2: Fitted intermittency parameter of the log-normal model and values following from the sixth-order scaling exponents of the angular and radial structure functions. Also listed are the standard errors of the scaling exponents following from power-law fits to the structure functions (see paper I).

$t$ [s]	Ka = 1		Ka = 10		Ka = 31.6	
	$P_{\text{DDT}}^{(\text{ang})}$	$P_{\text{DDT}}^{(\text{rad})}$	$P_{\text{DDT}}^{(\text{ang})}$	$P_{\text{DDT}}^{(\text{rad})}$	$P_{\text{DDT}}^{(\text{ang})}$	$P_{\text{DDT}}^{(\text{rad})}$
0.6	$3.0 \times 10^{-7}$	$4.8 \times 10^{-7}$	$\sim 0$	$\sim 0$	$\sim 0$	$\sim 0$
0.7	0.045	0.050	0.0024	0.0026	$4.2 \times 10^{-4}$	$4.8 \times 10^{-4}$
0.8	0.52	0.53	0.22	0.22	0.12	0.13
0.9	0.93	...	0.72	...	0.59	...

Table 3: Effective probability of a DDT inferred from equation (7) for different values of the Karlovitz number.

$\text{Da}_{\text{crit}}$	$P_{\text{DDT}}^{(\text{ang})}$	$N_{\text{DDT}}^{(\text{ang})}$	$P_{\text{DDT}}^{(\text{rad})}$	$N_{\text{DDT}}^{(\text{rad})}$
$t = 0.7$ seconds, $N_{\text{K/RT}} \approx 6.1 \cdot 10^5$				
2.15	$\sim 0$	$\sim 0$	$\sim 0$	$\sim 0$
4.64	$\sim 0$	$\sim 0$	$\sim 0$	$\sim 0$
10.0	$\sim 0$	$\sim 0$	$\sim 0$	$\sim 0$
21.5	$1.1 \times 10^{-8}$	$7.0 \times 10^{-3}$	$\sim 0$	$\sim 0$
46.4	$4.4 \times 10^{-6}$	2.7	$4.1 \times 10^{-6}$	2.5
100	$7.6 \times 10^{-5}$	$4.7 \times 10^1$	$8.6 \times 10^{-5}$	$5.3 \times 10^1$
$t = 0.8$ seconds, $N_{\text{K/RT}} \approx 1.7 \cdot 10^6$				
2.15	0.0021	$3.9 \times 10^3$	0.0022	$3.7 \times 10^3$
4.64	0.0061	$1.1 \times 10^4$	0.0061	$1.1 \times 10^4$
10.0	0.013	$2.4 \times 10^4$	0.014	$2.4 \times 10^4$
21.5	0.026	$4.8 \times 10^4$	0.027	$4.7 \times 10^4$
46.4	0.046	$8.4 \times 10^4$	0.047	$8.2 \times 10^4$
100	0.076	$1.4 \times 10^5$	0.077	$1.3 \times 10^5$
$t = 0.9$ seconds, $N_{\text{K/RT}} \approx 4.1 \cdot 10^6$				
2.15	0.04	$1.8 \times 10^5$	...	...
4.64	0.10	$3.9 \times 10^5$	...	...
10.0	0.15	$6.3 \times 10^5$	...	...
21.5	0.22	$8.8 \times 10^5$	...	...
46.4	0.28	$1.2 \times 10^6$	...	...
100	0.36	$1.5 \times 10^6$	...	...

Table 4: Dependence of the effective probability of a DDT and the expectation value of the number of DDTs on the critical Damköhler number for several instants.

$\mu$	$v'_{\text{min}} = 0 \text{ km s}^{-1}$		$v'_{\text{min}} = 200 \text{ km s}^{-1}$		$v'_{\text{min}} = 500 \text{ km s}^{-1}$	
	$P_{\text{DDT}}$	$N_{\text{DDT}}$	$P_{\text{DDT}}$	$N_{\text{DDT}}$	$P_{\text{DDT}}$	$N_{\text{DDT}}$
0.05	0.155	$6.34 \times 10^5$	$6.4 \times 10^{-9}$	$2.6 \times 10^{-2}$	$\sim 0$	$\sim 0$
0.1	0.154	$6.30 \times 10^5$	$5.8 \times 10^{-6}$	$2.4 \times 10^1$	$\sim 0$	$\sim 0$
0.15	0.153	$6.25 \times 10^5$	$5.8 \times 10^{-5}$	$2.4 \times 10^2$	$\sim 0$	$\sim 0$
0.2	0.152	$6.20 \times 10^5$	$1.8 \times 10^{-4}$	$7.5 \times 10^2$	$1.1 \times 10^{-9}$	$4.4 \times 10^{-3}$

Table 5: Dependence of the effective probability of a DDT and the expectation value of the number of DDTs on the intermittency parameter  $\mu$  of the log-normal model and the minimal velocity fluctuation  $v'_{\text{min}}$  for  $t = 0.9$  seconds.

Da <sub>crit</sub>	$v'_{\min} = 200 \text{ km s}^{-1}$		$v'_{\min} = 500 \text{ km s}^{-1}$		$v'_{\min} = 1000 \text{ km s}^{-1}$	
	$P_{\text{DDT}}$	$N_{\text{DDT}}$	$P_{\text{DDT}}$	$N_{\text{DDT}}$	$P_{\text{DDT}}$	$N_{\text{DDT}}$
$t = 0.7 \text{ seconds, } N_{\text{K/RT}} \approx 6.1 \cdot 10^5$						
2.15	$\sim 0$	$\sim 0$	$\sim 0$	$\sim 0$	$\sim 0$	$\sim 0$
4.64	$3.7 \times 10^{-9}$	$2.3 \times 10^{-3}$	$2.3 \times 10^{-9}$	$1.4 \times 10^{-3}$	$\sim 0$	$\sim 0$
10.0	$3.9 \times 10^{-7}$	$2.4 \times 10^{-1}$	$4.2 \times 10^{-8}$	$2.6 \times 10^{-2}$	$\sim 0$	$\sim 0$
21.5	$5.9 \times 10^{-6}$	3.6	$2.1 \times 10^{-7}$	$1.3 \times 10^{-1}$	$\sim 0$	$\sim 0$
46.4	$3.0 \times 10^{-5}$	$1.9 \times 10^1$	$6.6 \times 10^{-7}$	$4.0 \times 10^{-1}$	$1.7 \times 10^{-9}$	$1.0 \times 10^{-3}$
100	$9.5 \times 10^{-5}$	$5.8 \times 10^1$	$1.8 \times 10^{-6}$	1.1	$4.5 \times 10^{-9}$	$2.8 \times 10^{-3}$
$t = 0.8 \text{ seconds, } N_{\text{K/RT}} \approx 1.7 \cdot 10^6$						
2.15	$3.5 \times 10^{-4}$	$6.2 \times 10^2$	$6.2 \times 10^{-6}$	$1.1 \times 10^1$	$3.9 \times 10^{-8}$	$6.8 \times 10^{-2}$
4.64	$9.9 \times 10^{-4}$	$1.7 \times 10^3$	$1.6 \times 10^{-5}$	$2.8 \times 10^1$	$9.8 \times 10^{-8}$	$1.7 \times 10^{-1}$
10.0	$2.0 \times 10^{-3}$	$3.5 \times 10^3$	$3.1 \times 10^{-5}$	$5.3 \times 10^1$	$1.8 \times 10^{-7}$	$3.2 \times 10^{-1}$
21.5	$3.5 \times 10^{-3}$	$6.1 \times 10^3$	$5.1 \times 10^{-5}$	$8.9 \times 10^1$	$3.0 \times 10^{-7}$	$5.1 \times 10^{-1}$
46.4	$5.6 \times 10^{-3}$	$9.8 \times 10^3$	$7.9 \times 10^{-5}$	$1.4 \times 10^2$	$4.5 \times 10^{-7}$	$7.8 \times 10^{-1}$
100	$8.5 \times 10^{-3}$	$1.5 \times 10^4$	$1.2 \times 10^{-4}$	$2.0 \times 10^2$	$6.3 \times 10^{-7}$	1.1
$t = 0.9 \text{ seconds, } N_{\text{K/RT}} \approx 4.1 \cdot 10^6$						
2.15	$6.1 \times 10^{-4}$	$2.5 \times 10^3$	$1.2 \times 10^{-6}$	4.8	$\sim 0$	$\sim 0$
4.64	$1.3 \times 10^{-3}$	$5.3 \times 10^3$	$2.4 \times 10^{-6}$	9.9	$1.2 \times 10^{-9}$	$5.0 \times 10^{-3}$
10.0	$2.0 \times 10^{-3}$	$8.3 \times 10^3$	$3.8 \times 10^{-6}$	$1.6 \times 10^1$	$1.9 \times 10^{-9}$	$7.8 \times 10^{-3}$
21.5	$2.8 \times 10^{-3}$	$1.2 \times 10^4$	$5.2 \times 10^{-6}$	$2.1 \times 10^1$	$2.6 \times 10^{-9}$	$1.1 \times 10^{-2}$
46.4	$3.7 \times 10^{-3}$	$1.5 \times 10^4$	$6.7 \times 10^{-6}$	$2.8 \times 10^1$	$3.3 \times 10^{-9}$	$1.4 \times 10^{-2}$
100	$4.6 \times 10^{-3}$	$1.9 \times 10^4$	$8.3 \times 10^{-6}$	$3.4 \times 10^1$	$4.0 \times 10^{-9}$	$1.6 \times 10^{-2}$

Table 6: Dependence of the effective probability of a DDT and the expectation value of the number of DDTs on the critical Damköhler number corresponding to Table 4 for a non-log-normal distribution of turbulent velocity fluctuations (Röpke 2007).